

## Lead-zirconate-titanate-based piezoelectric micromachined switch

S. J. Gross,<sup>a)</sup> S. Tadigadapa, and T. N. Jackson

*Department of Electrical Engineering, The Pennsylvania State University,  
University Park, Pennsylvania 16802*

S. Trolier-McKinstry

*Department of Materials Science & Engineering, The Pennsylvania State University,  
University Park, Pennsylvania 16802*

Q. Q. Zhang

*Geospace Research, El Segundo, California 90245*

(Received 27 November 2002; accepted 3 May 2003)

A piezoelectric microelectromechanical switch actuated by lead zirconate titanate (PZT) is reported. A PZT unimorph cantilever actuator, fabricated on a sacrificial polysilicon layer and released using a xenon difluoride dry etch, was used to realize the switch. The PZT thin film was poled and driven with interdigitated electrodes to exploit the  $d_{33}$  coefficient for switching actuation. Preliminary dc and rf switching characteristics are reported. Measurements indicate a fast switching “on” time of  $<2 \mu\text{s}$  and “off” time of  $2 \mu\text{s}$  at an actuation voltage of  $<40 \text{ V}$ . An on/off isolation of  $>25 \text{ dB}$  was achieved up to  $100 \text{ MHz}$ . © 2003 American Institute of Physics. [DOI: 10.1063/1.1589192]

In this letter, a piezoelectric microelectromechanical switch is presented. The switch uses a  $\text{PbZr}_{0.52}\text{Ti}_{0.48}\text{O}_3$  (PZT) cantilever actuator in the  $d_{33}$  mode to achieve switching operation and high speed. This work is motivated by the recent advances that have made microelectromechanical systems (MEMS) rf components attractive as replacements for conventional crystal resonators, filters, and semiconductor switches.<sup>1</sup> Application areas that stand to benefit from these emerging rf MEMS technologies include satellite and wireless communication systems, commercial and military radar, global positioning systems, and instrumentation systems.<sup>2</sup> Typical semiconductor switches, such as GaAs field-effect transistors and  $p-i-n$  diodes, currently used in these applications exhibit high insertion losses ( $S_{21}$ ) of 1–2 dB or greater, and poor isolation in the off state due to parasitics.<sup>3</sup> On the contrary, MEMS switches have demonstrated significant improvements with insertion losses of less than 0.1 dB up to 40 GHz and very high isolation ( $>27 \text{ dB}$ ) when turned off.<sup>2,3</sup> In addition, MEMS switches typically consume negligible power during each switching cycle. Signal switching is accomplished by the mechanical deflection of a suspended structure yielding a metal-to-metal contact or capacitive coupling. Various actuation methods have been investigated including electrostatic,<sup>4</sup> electromagnetic,<sup>5</sup> thermal, and piezoelectric.<sup>6</sup> At present, the majority of MEMS switches employ electrostatic actuation. However, electrostatic actuation is a nonlinear mechanism, and usually requires high voltages to operate, especially if high-frequency operation is desired. Switching times below  $10 \mu\text{s}$  typically require greater than  $50 \text{ V}$ .<sup>7</sup>

Exploiting an alternative actuation method such as the converse piezoelectric effect is expected to lead to a substantial improvement in device performance. The energy density available in ferroelectric thin films such as PZT is at least an order of magnitude greater than with electrostatics, and sub-

sequently the potential for conversion to mechanical work is much greater.<sup>8</sup> This difference can lead to lower actuation voltages and faster switching speeds. Normally-off electrostatic switches rely upon the elastic restoring force of the moving structure for achieving the off state. Since the restoring force is smaller than the closing force, opening is slower, leading inevitably to design trade-offs. Piezoelectric strains can be either positive or negative (within the limits set by the reorientation of the domain state in a ferroelectric film) and can therefore be used actively to turn the switch off as well as on. This characteristic allows the design of larger contacts for high-power capability as well as improved reliability due to mitigated stiction effects.

Ferroelectric PZT thin films with high piezoelectric coefficient  $d_{33}=120 \text{ pC/N}$  have been used as the active material.<sup>9,10</sup> Despite the high coefficient, the strain generated by these perovskite ceramic thin films is typically small, on the order of 0.1%. Therefore, a bending structure is used to increase the deflection at the expense of the force. Figure 1(a) shows a schematic representation of the current unimorph (heterogeneous bimorph) design, and Fig. 1(b) shows a scanning electron microscope (SEM) image of a fabricated switch with dc transmission lines. The unimorph is composed of a PZT active layer on top of a passive stack of zirconia ( $\text{ZrO}_2$ ) and silicon nitride ( $\text{Si}_3\text{N}_4$ ). With the interdigitated (IDT) electrode configuration the PZT is poled in the transverse direction and actuated in the  $d_{33}$  mode.<sup>11,12</sup> The electrode width is  $3 \mu\text{m}$  with a separation of  $6 \mu\text{m}$ . The maximum deflection and blocking force in a unimorph are achieved by optimizing the thickness ratio of the passive/active materials.<sup>13</sup> Residual stresses in deposited thin films often result in out-of-plane bending of the cantilevers, which adversely affects performance, and if severe enough, can prevent switch closure completely. Therefore, the structures were stress compensated by controlling the PZT thickness.

Fabrication begins with an insulating substrate, in this case an oxidized ( $1.5\text{-}\mu\text{m}$ ) silicon wafer. A sacrificial poly-

<sup>a)</sup>Electronic mail: sjpg12@psu.edu

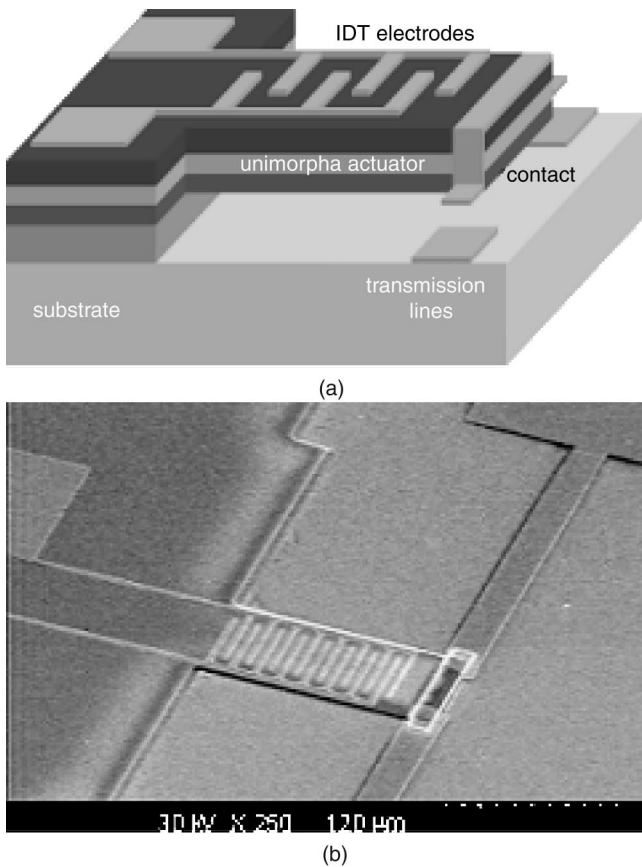


FIG. 1. (a) Schematic illustration of unimorph switch and (b) SEM image of 130- $\mu\text{m}$  cantilever switch with transmission lines.

silicon ( $2\ \mu\text{m}$ ) is deposited by low-pressure chemical vapor deposition methods, and a thin thermal oxide ( $50\ \text{nm}$ ) is grown to act as a barrier layer. Low-stress ( $400\text{-MPa}$ ) silicon nitride ( $0.5\ \mu\text{m}$ ) is deposited as the structural material. A thin silicon oxide ( $50\ \text{nm}$ ) is sputter deposited to promote adhesion of the remaining layers with the nitride. A buffer layer of  $0.3\text{-}\mu\text{m}$  zirconia and  $0.23\text{-}\mu\text{m}$  PZT are spun on using sol-gel techniques. The material stack is then patterned using a combination of ion milling and reactive ion etching. The contact at the end of the cantilever is deposited by sputter deposition and patterned by lift-off. The field polysilicon is then etched away, terminating on the thick substrate oxide. A blanket Cr/Au is sputter deposited at an angle off normal to coat below the contact. This blanket layer is etched to define the transmission lines and IDT electrodes. The final structure release is attained by dry etching the sacrificial polysilicon in gaseous  $\text{XeF}_2$ .<sup>14</sup> A more detailed account of the fabrication process is presented in Ref. 15.

The completed switches were first tested using  $2\ \text{V}$  dc on the transmission lines, with the switch shunting the output signal to ground when on. A buffer amplifier is used to provide a high input impedance and a  $300\text{-k}\Omega$  resistor is used to limit the current passed through the contacts. Figure 2 shows the switching response to a  $1\text{-Hz}$   $0\text{--}20\text{-V}$  square wave input superimposed on  $10\ \text{V}$  dc. The oscilloscope trace demonstrates that the switch opens and closes concurrently with the applied signal. Closer examination reveals a  $2\text{-}\mu\text{s}$  switching time between the off state and the on state, and the same for switching off. The next series of tests were conducted to

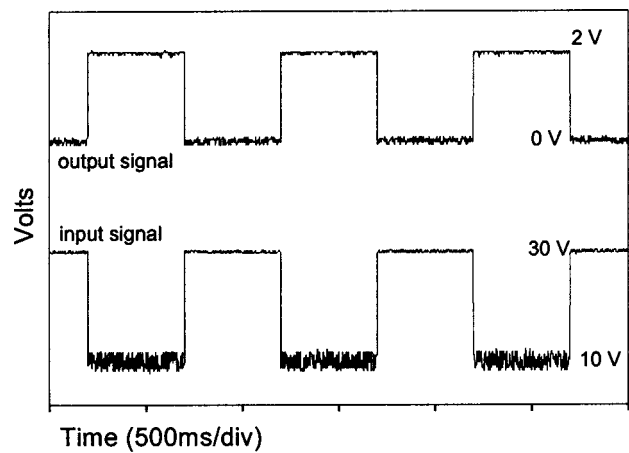


FIG. 2. Switching response (top) to a  $1\text{-Hz}$   $20\text{-V}_{\text{peak-peak}} + 10\text{-V}_{\text{dc}}$  square wave (bottom).

observe the switching behavior when actuated by short pulses. Figure 3(a) shows an oscilloscope trace of a  $30\text{-V}$ ,  $4\text{-}\mu\text{s}$  pulse (top) and the switch response (bottom). The noise seen on the bottom trace during switching is a result of coupling between the IDT electrodes and contact. Figure 3(b) shows the response to a pulse of higher voltage but same duration:  $50\ \text{V}$ ,  $4\ \mu\text{s}$ . As can be seen, the switching on time is decreased from  $2.5$  to about  $1.5\ \mu\text{s}$ , while the switching off time remains constant. Preliminary results using a gain-phase analyzer (HP4194A) have demonstrated that signals up to

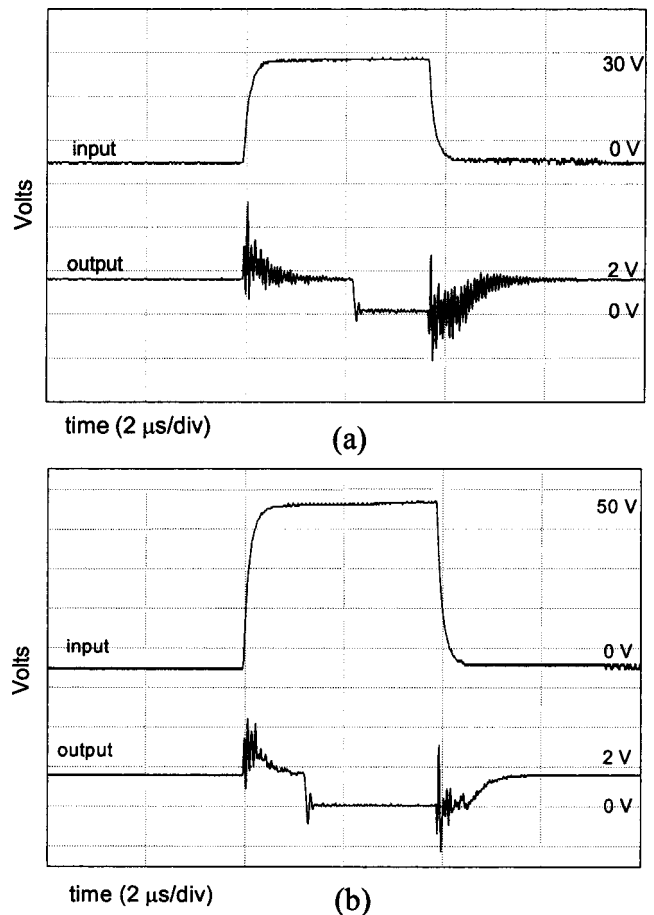


FIG. 3. Switching response (bottom trace) to  $30\text{-V}$  (a) and  $50\text{-V}$  (b)  $2\text{-}\mu\text{s}$  pulse (top trace).

100 MHz can be switched, with approximately 30 dB of isolation between the on and off states.

These results correspond to a device with a cantilever length of 230  $\mu\text{m}$  (27 IDT electrodes), a width of 100  $\mu\text{m}$  and a 1.1- $\mu\text{m}$  thickness. The measured fundamental resonance frequency,  $f_0=19$  kHz, matches to within 10% of theory. An analysis of the switching time begins with a dynamic model for a one-degree-of-freedom system. The equation of motion is given as

$$F = m \frac{d^2 z}{dt^2} + b \frac{dz}{dt} + kz, \quad (1)$$

where  $m$  is the mass,  $z$  is the position of the tip at time  $t$ ,  $k$  is the spring constant of the cantilever, and  $F$ , the internal force, is generated by the piezoelectric effect. All forms of damping, including squeeze damping, have been ignored;  $b=0$ .<sup>2</sup> The force is modeled as a step function by ignoring the IDT electrode capacitance charging time and material mechanical relaxation. With the tip displacement and velocity set to zero as initial conditions, the particular solution is given as

$$z(t) = z_0 - z_0 \cos(\omega_n t), \quad (2)$$

where  $z_0$  is the static deflection and the natural frequency  $\omega_n = 2\pi f_0$ . The time ( $\tau_{\text{on}}$ ) required to close the gap( $\delta$ ) between the contact and the transmission lines can be obtained from Eq. (2):

$$\tau_{\text{on}} = \frac{1}{2\pi f_0} \cos^{-1} \left( 1 - \frac{\delta}{z_0} \right). \quad (3)$$

For this device,  $\delta=1$   $\mu\text{m}$ ,  $z_0=13$   $\mu\text{m}$  at 50 V (theory), and, by Eq. (3),  $\tau_{\text{on}}=3.3$   $\mu\text{s}$ , which is comparable to the measured value. Since  $z_0$  is proportional to the driving voltage, the larger the driving voltage, the shorter  $\tau_{\text{on}}$ , which is consistent with experiments. The turn-off time, however, is solely determined by the gap spacing and the natural fre-

quency. Fast switching compared with resonance frequencies has also been observed in electrostatic switches.<sup>2</sup>

In conclusion, we have fabricated and tested a transverse mode piezoelectric microswitch based on ferroelectric PZT thin films. A robust fabrication process using ion milling and dry release in  $\text{XeF}_2$  to avoid stiction-related problems has been developed. Initial measurements have demonstrated relatively high switching speeds (1–2  $\mu\text{s}$ ), and  $\sim 30$ -dB isolation between on and off states at 100 MHz. The actuation voltage of these piezoelectric switches is expected to be lower with better stress compensation, more closely spaced IDT electrodes, or by the use of a bimorph design. Improved performance at higher frequencies is expected with rf transmission lines and by using insulating substrates.

The authors gratefully acknowledge support from the U.S. Army and the Northrop Grumman Corporation.

<sup>1</sup>C. T.-C. Nguyen, *Proceedings of the Sensors Exposition*, 19–21 May 1998, p. 447.

<sup>2</sup>G. Rebeiz and J. Muldavin, *IEEE Microwave Mag.* **2**, 59 (2001).

<sup>3</sup>J. J. Yao, *J. Micromech. Microeng.* **10**, R9 (2000).

<sup>4</sup>K. E. Petersen, *IBM J. Res. Dev.* **23**, 376 (1979).

<sup>5</sup>M. Ruan, J. Shen, C. B. Wheeler, *The 14th IEEE International Conference on Micro Electro Mechanical Systems*, 2001, p. 224.

<sup>6</sup>C. M. Beck, M. M. Ahmed, C. J. Brierley, A. P. Needham, and S. P. Marsh, *IEEE Intr. Microwave Symposium*, 2000.

<sup>7</sup>E. Brown, *IEEE Trans. Microwave Theory Tech.* **46**, 1868 (1998).

<sup>8</sup>A. M. Flynn, L. S. Tavrow, S. F. Bart, R. A. Brooks, D. J. Ehrlich, K. R. Udayakumar, and L. E. Cross, *J. Microelectromech. Syst.* **1**, 44 (1992).

<sup>9</sup>L. E. Cross and S. Trolier-McKinstry, *Encl. Appl. Phys.* **21**, 429 (1997).

<sup>10</sup>D. Polla and Lorraine Francis, *Annu. Rev. Mater. Sci.* **28**, 563 (1998).

<sup>11</sup>B. Xu, R. G. Polcawich, S. Trolier-McKinstry, Y. Ye, L. E. Cross, J. J. Bernstein, and R. Miller, *Appl. Phys. Lett.* **75**, 4180 (1999).

<sup>12</sup>Q. Zhang, S. J. Gross, S. Tadigadapa, T. N. Jackson, F. T. Djuth, D. M. Machuga, and S. Trolier-McKinstry, *Sens. Actuators A* **105**, 91 (2003).

<sup>13</sup>Q.-M. Wang, X.-H. Du, B. Xu, and L. E. Cross, *IEEE Trans. Ultrason. Ferroelectr. Freq. Control* **46**, 638 (1999).

<sup>14</sup>P. B. Chu, J. T. Chen, R. Yeh, G. Lin, J. C. P. Huang, B. A. Warneke, and K. S. J. Pister, *IEEE International Conference on Transducers'97*, 1997.

<sup>15</sup>S. J. Gross, Q. Q. Zhang, S. Tadigadapa, S. Trolier-McKinstry, T. N. Jackson, and F. Djuth, *Proc. SPIE* **558**, 72 (2001).